An investigation of the local environments of tin in tin-doped α-Fe$_2$O$_3$

An investigation of the local environments of tin in tin-doped α-Fe$_2$O$_3$

Frank J Berry†, Alberto Bohórquez†¶, Örn Helgason‡, Jianzhong Jiang§,
Julia McManus†, Elaine Moore†, Michael Mortimer†,
Frederick Mosselmans‖ and Steen Mørup§

† Department of Chemistry, The Open University, Walton Hall, Milton Keynes MK7 6AA, UK
‡ Science Institute, University of Iceland, Dunhagi 3, IS-107 Reykjavik, Iceland
§ Department of Physics, Building 307, Technical University of Denmark, DK-2800 Lyngby, Denmark
‖ Daresbury Laboratory, Daresbury, Warrington WA4 4AD, UK

Abstract. The extended x-ray absorption fine structure (EXAFS) recorded from tin-doped α-Fe$_2$O$_3$, prepared by the mechanical milling of tin dioxide and α-Fe$_2$O$_3$ and by the hydrothermal processing of iron- and tin-containing precipitates, can be interpreted in terms of a model in which tin occupies both substitutional octahedral sites and the interstitial octahedral sites in the corundum-related α-Fe$_2$O$_3$ structure. The EXAFS and ^{119}Sn Mössbauer spectra suggest that structural models derived from x-ray powder diffraction data do not adequately describe the complexity of the local environment of tin in α-Fe$_2$O$_3$. In particular, the EXAFS and ^{119}Sn Mössbauer spectra recorded from materials made by mechanical milling show evidence of more disorder. The ^{119}Sn Mössbauer spectra also indicate that the degree of order in the materials made by both methods is far from perfect and that the microstructural defects are highly sensitive to tin content and the preparative method.

1. Introduction

The structure of α-Fe$_2$O$_3$ is related to that of corundum and involves the Fe^{3+} ions being distributed in an ordered fashion in 2/3 of the octahedral sites within a framework of hexagonally close-packed O^{2-} ions. Chains of face-sharing octahedra are directed along the c-axis, and the Fe^{3+} ions within each chain form pairs separated by an empty interstitial site, as shown in figure 1. The changes in the electrical, magnetic, and other physical properties of α-Fe$_2$O$_3$, which result from the doping of α-Fe$_2$O$_3$ with tin, have been the subject of interest for many years [1–5]. It has generally been assumed that the dopant tin ions substitute for Fe^{3+} in the corundum-related structure of α-Fe$_2$O$_3$ with the consequent formation of cationic and anionic vacancies.

The microstructure of tin-doped α-Fe$_2$O$_3$, prepared by mechanical milling, was recently examined by Jiang *et al* (1997) using Rietveld structure refinement of x-ray powder diffraction data, and the results were interpreted in terms of the Sn^{4+} ions occupying interstitial octahedral sites in the α-Fe$_2$O$_3$ lattice [6]. Simultaneously, materials prepared by hydrothermal methods (Berry *et al* 1997 [7]) were also investigated by Rietveld structure refinement of the x-ray powder diffraction data and the results interpreted in terms of tin partially substituting at the

¶ Permanent address: Departamento de Fisica, Universidad del Valle, AA25360 Cali, Colombia.
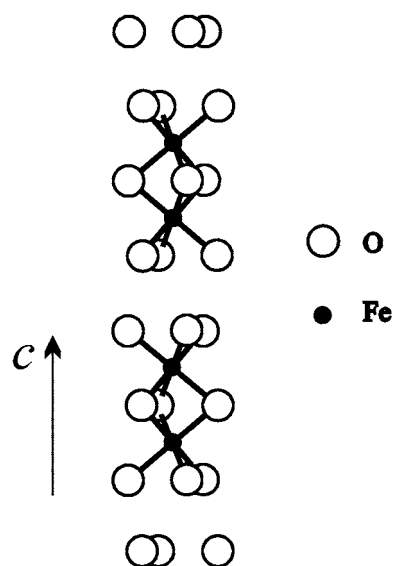
Figure 1. Linking of FeO_6 along c in α-Fe_2O_3.

octahedral lattice sites and also occupying the vacant interstitial octahedral sites in the α-Fe_2O_3 lattice.

In an attempt to investigate further this apparent difference in the microstructural properties of tin doped α-Fe_2O_3 prepared by different techniques, we have examined the environment of the tin in α-Fe_2O_3 using x-ray absorption fine structure (EXAFS) and ^{119}Sn Mössbauer spectroscopy. These techniques are both well suited to the investigation of the local environment of the dopant ion.

2. Experimental details

Tin-doped α-Fe_2O_3 was prepared by milling a mixture of α-Fe_2O_3 (particle size $\sim$10 μm) and SnO_2 (particle size $\sim$10 μm) in containers open to air using a planetary ball mill (Fritsch Pulverisette 5) with tungsten carbide vials and balls. The milling intensity was 200 rpm and a ball-to-powder weight ratio of 20:1 was selected. Tin-doped α-Fe_2O_3 was also prepared by precipitating aqueous mixtures of iron(III) chloride hexahydrate and tin(IV) chloride with aqueous ammonia and hydrothermally processing the precipitates in a Teflon®-lined autoclave at 200 °C and 15 atm pressure for 5 hours. The products were removed by filtration and washed with 95% ethanol until no chloride ions were detected by silver nitrate solution. The products were dried under an infrared lamp. The monophasic nature of products was confirmed by x-ray powder diffraction as previously described [6, 7].

The tin K-edge EXAFS measurements were performed at the Synchrotron Radiation Source, Daresbury Laboratory, UK, with an average current of 200 mA at 2 GeV. The data were collected at 77 K in transmission geometry on Station 9.2 with a Si(220) double crystal monochromator that was detuned to 70% of the maximum intensity to remove the harmonic. Ion chambers were filled with noble gases so as to absorb *ca* 20% and *ca* 80% of the beam in the first and second chambers, respectively. The energy resolution of the monochromator is *ca* 5 eV at the tin K-edge. The samples were examined as pressed discs. The raw data were reduced using the SRS programs EXCALIB and EXBACK, EXAFS data

Table 1. Best fit parameters to the tin K-edge EXAFS recorded from 5% tin-doped α-Fe$_2$O$_3$.

Method of preparation	Fitting model	Fit index R (and reduced χ^2)	Atom type	Coordination number	Tin–atom distance (Å)±1%	$2\sigma^2$ (Å^2) ±10%
Milling	Jiang [6]	19.80	O	5	2.05	0.006
		(12.4)	Fe	6	3.10	0.035
			O	6	3.45	0.027
Milling	Berry [7]	13.42	O[a]	6	2.02	0.007
		(9.0)	Fe	3	3.14	0.020
			Fe	3	3.59	0.020
			O	3	3.35	0.005
			O	3	3.80	0.005
			O[b]	6	2.10	0.007
			Fe	6	3.04	0.020
			O	6	3.49	0.005
Hydrothermal	Jiang [6]	26.21	O	5	2.05	0.005
		(16.8)	Fe	6	3.06	0.020
			O	6	3.42	0.007
Hydrothermal	Berry [7]	19.35	O[a]	6	2.02	0.003
		(14.7)	Fe	3	3.11	0.005
			Fe	3	3.50	0.005
			O	3	3.38	0.002
			O	3	3.70	0.002
			O[b]	6	2.13	0.003
			Fe	6	3.00	0.005
			O	6	3.67	0.002

[a] Data for substitutional tin.
[b] Data for interstitial tin.

analyses were performed using the program EXCURV98 [8]. Phase shifts using Muffin-Tin potentials were calculated *ab initio* using Hedin–Lundqvist exchange potentials and von Barth ground state potentials. The fit index R that is quoted in tables 1 and 2 is defined by $R = \sum_i [(1/(\sigma_i))(\text{experiment}(i) - \text{theory}(i)] * 100\%$ where $1/(\sigma_i) = [k(i)]^3/(\sum_i [k(i)]^3 \, \text{experiment}(i))$. The reduced χ^2 values, also quoted in tables 1 and 2, take into account the number of parameters refined in fitting the data to a specific model.

In fitting the model proposed by Berry *et al* [7], two thirds of the tin ions were considered to occupy substitutional iron sites and the remaining third to occupy interstitial sites. The number of free parameters was restrained by treating the Sn–O octahedra as one shell and setting several of the Debye–Waller factors to be equal. In particular, the following pairs of Debye-Waller factors were refined as one parameter: those of the first shell oxygen atoms in each cluster, those of the two iron next-nearest neighbour shells in the exchanged site, and those of the oxygen atoms at *ca* 3.5 Å from the exchanged tin. This approach meant that twelve parameters corresponding to the distinct dopant sites were refined in fitting the model to the datasets, while seven were used when fitting the single dopant site model of Jiang *et al* [6]. Coordination numbers deduced from the models were not refined and the value of AFAC (amplitude reduction factor) used was 1.

[119]Sn Mössbauer spectra were recorded at 298 K and 17 K with a conventional constant acceleration spectrometer in transmission geometry and a 5mCi Ba[119m]SnO$_3$ source. The isomer shifts are given relative to that of α-Fe at room temperature. The linewidth of the calibration spectrum was 0.24 (1) mms^{-1}.

Table 2. Best fit parameters to the tin K-edge EXAFS recorded from 11% tin-doped α-Fe$_2$O$_3$.

Method of preparation	Fitting model	Fit index R (and reduced χ^2)	Atom type	Coordination number	Tin–atom distance (Å)±1%	$2\sigma^2$(Å^2) ±10%
Milling	Jiang [6]	21.34	O	5	2.04	0.006
		(10.8)	Fe	6	3.08	0.030
			O	6	3.44	0.021
Milling	Berry [7]	16.92	O[a]	6	2.02	0.006
		(6.0)	Fe	3	3.11	0.019
			Fe	3	3.41	0.019
			O	3	3.42	0.008
			O	3	3.55	0.008
			O[b]	6	2.11	0.006
			Fe	6	3.05	0.019
			O	6	3.55	0.008
Hydrothermal	Jiang [6]	21.48	O	5	2.05	0.005
		(10.0)	Fe	6	3.08	0.027
			O	6	3.45	0.025
Hydrothermal	Berry [7]	14.03	O[a]	6	2.02	0.005
		(7.3)	Fe	3	3.07	0.019
			Fe	3	3.43	0.019
			O	3	3.53	0.005
			O	3	3.53	0.005
			O[a]	6	2.11	0.005
			Fe	6	3.08	0.019
			O	6	3.83	0.005

[a] Data for substitutional tin.
[b] Data for interstitial tin.

In fitting the ^{119}Sn Mössbauer spectra consideration was given to the possibilities resulting from the different models. According to the model proposed by Jiang *et al* [6], Sn^{4+} ions in samples of low tin content generally have only Fe^{3+} ions as nearest cation neighbours. Although the Sn^{4+} ion itself is nonmagnetic, its nucleus can sense a magnetic hyperfine field by supertransferred hyperfine interaction (STHI) with Fe^{3+} ions in the α-Fe$_2$O$_3$ structure. In this situation the ^{119}Sn Mössbauer spectrum would be expected to be dominated by a single sextet. In materials with increasing tin concentration a new sextet, or distribution of sextets, with a reduced magnetic hyperfine field resulting from Sn^{4+} ions with one or more nearest neighbour Sn^{4+} ions might also be expected.

In the case of Berry's model [7] the microstructure at the dopant ion may be best described as a 'tin triplet', in which three Sn^{4+} ions form a chain along the *c*-axis. In this case two sextets in the ^{119}Sn Mössbauer spectrum with different hyperfine fields might be expected. The component with the larger magnetic hyperfine field would correspond to the two Sn^{4+} ions in substitutional octahedral sites with one tin neighbour, while the sextet with smaller field would represent the Sn^{4+} ions in the interstitial sites with two tin neighbours. Furthermore, according to this model, a constant area ratio, close to 2:1 in favour of the component with larger magnetic field, would be expected in materials in which the tin concentration is sufficiently small to avoid interaction between different 'tin-triplets'.

It should also be appreciated that in both models Sn^{4+} ions in the surface of the particles would also be expected to experience a small magnetic hyperfine interaction, although this would only be of importance in the case of ball milled samples where the particles are smaller.

3. Results

The tin K-edge EXAFS recorded from 5% tin-doped α-Fe$_2$O$_3$ prepared by milling and hydrothermal methods and fitted to the models of Jiang *et al* [6] and Berry *et al* [7] are shown in figure 2. The best fit parameters obtained from the two models are collected in table 1. Both the R values and the reduced χ^2 values are lower when the model [7] involving the occupation by tin of both substitutional and interstitial sites is applied to both materials.
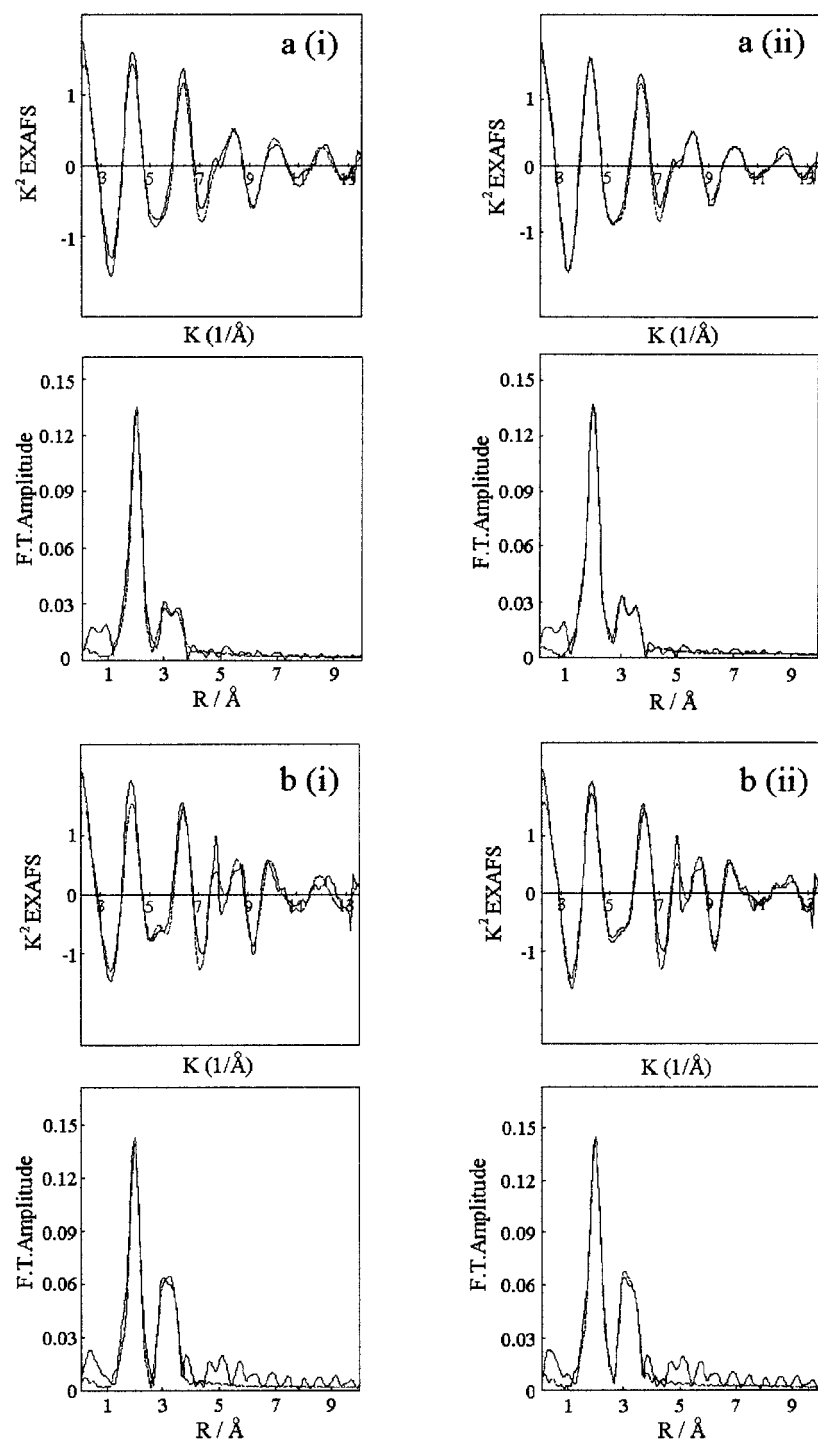
The tin K-edge EXAFS recorded from 11% tin-doped α-Fe$_2$O$_3$ prepared by both methods and fitted to both models are shown in figure 3. The best fit parameters are collected in table 2. The R values are again lower when the data are fitted to the model [7] involving tin occupying both substitutional and interstitial sites.

The ^{119}Sn Mössbauer spectra recorded at 298 K for three samples of tin-doped α-Fe$_2$O$_3$ with low tin content are shown in figure 4. Three sextets with broad linewidths (and nearly zero quadrupole shift) and a doublet (with an isomer shift of 0.15 mms^{-1} and a quadrupole splitting of 0.56 mms^{-1}) were needed to obtain a reasonable fit to the data. The results indicated that fitting the spectra to a distribution of hyperfine magnetic fields would be more appropriate. Hence, a model-independent distribution of hyperfine fields with a zero quadrupole splitting was applied [9]. The sextets of the field distribution were constrained to an area ratio of 3:2:1 with linewidths of 1.2 mms^{-1}. Steps of 0.3 T for the field distribution were used in the final version of the fitting procedure. Smaller steps only increased the 'smoothness' of the distribution without statistically improving the fit. The isomer shift was allowed to vary linearly with the magnetic hyperfine field. The results are shown in figure 5. The spectra recorded from all three samples showed (i) a maximum in the field distribution at about 12 T, (ii) identical structure above 4 T with small maxima at 5 T and 8 T. The reality of the two maxima was tested by making changes to the fitting procedure. Firstly, the sextet area ratio constraint of 3:2:1 was released. Small statistical improvements were obtained for a ratio of 2.7:1.9–1.88:1.1, but without a significant change of the area or position of the peaks at 5 T and 8 T. Secondly, a smoothing parameter in the distribution program [9] was allowed to increase to smear out the peaks. The value of χ^2 increased supporting the validity of the fit involving the two peaks at 5 T and 8 T.

The resolution of the distribution was superior in the spectra recorded from samples prepared by hydrothermal processing (2% tin in figure 5(a) and 4% tin in figure 5(c)) as compared to the spectrum recorded from the sample made by mechanical milling (figure 5(b)). It should be noted that the field distribution is unable to distinguish between a contribution from a doublet, as recorded from the first fitting procedure, and components from magnetic hyperfine interactions less than 2 T. We would comment that a spectrum recorded at 17 K from a sample containing 3% tin prepared by mechanical milling showed a very similar field distribution with, as expected for a measurement at 17 K, a small increase in the value of the hyperfine field.

4. Discussion

The two models by which the data have been interpreted are only slightly different and it is difficult to distinguish between the differences in local co-ordination by x-ray powder diffraction [6, 7]. The element specific nature of both EXAFS and ^{119}Sn Mössbauer spectroscopy allows the examination of the local environment of tin directly. The results show that a microstructure in which tin ions only substitute for Fe^{3+} in the corundum-related α-Fe$_2$O$_3$ structure is unlikely. The results suggest that tin-doped α-Fe$_2$O$_3$ prepared by both the mechanical milling of tin dioxide and α-Fe$_2$O$_3$ and by the hydrothermal processing of iron- and

Figure 2. K^2-weighted tin K-edge EXAFS and phase shifted Fourier transform recorded from 5% tin-doped α-Fe$_2$O$_3$ prepared by (a) mechanical milling and (b) hydrothermal processing and fitted to the models of (i) Jiang *et al* [6] and (ii) Berry *et al* [7]. The experimental data are shown by the solid line.
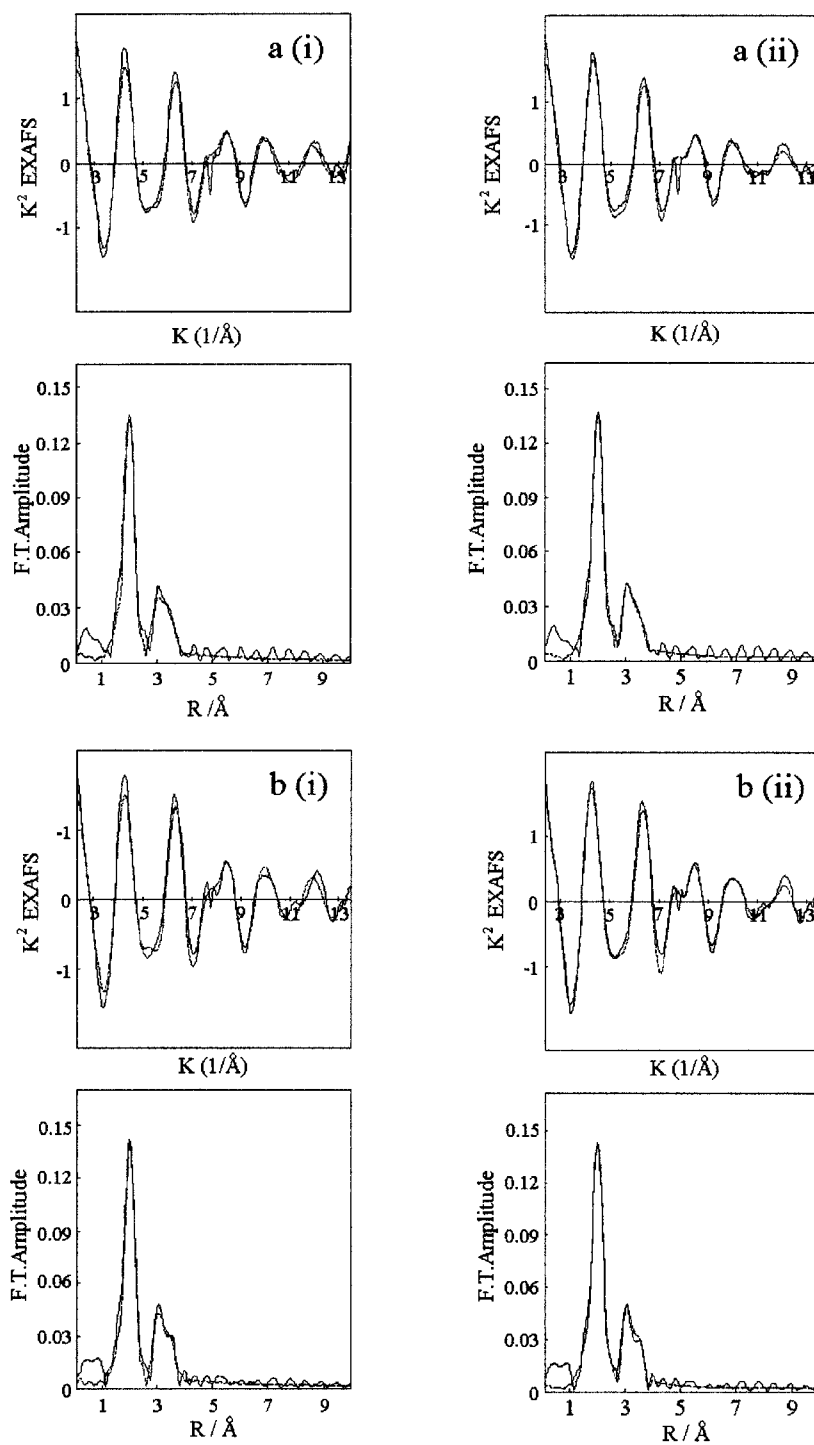
Figure 3. K^2-weighted tin K-edge EXAFS and phase shifted Fourier transform recorded from 11% tin-doped α-Fe$_2$O$_3$ prepared by (a) mechanical milling and (b) hydrothermal processing and fitted to the models of (i) Jiang *et al* [6] and (ii) Berry *et al* [7]. The experimental data are shown by the solid line.
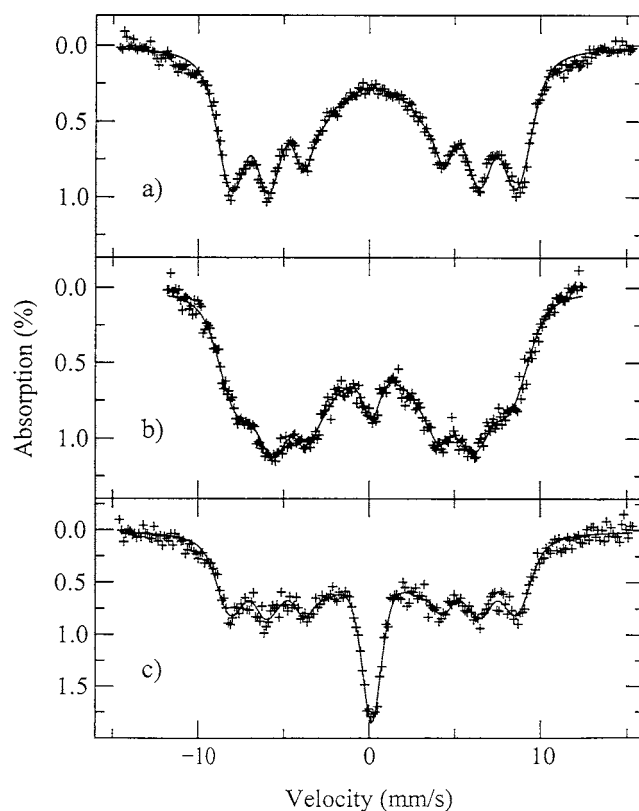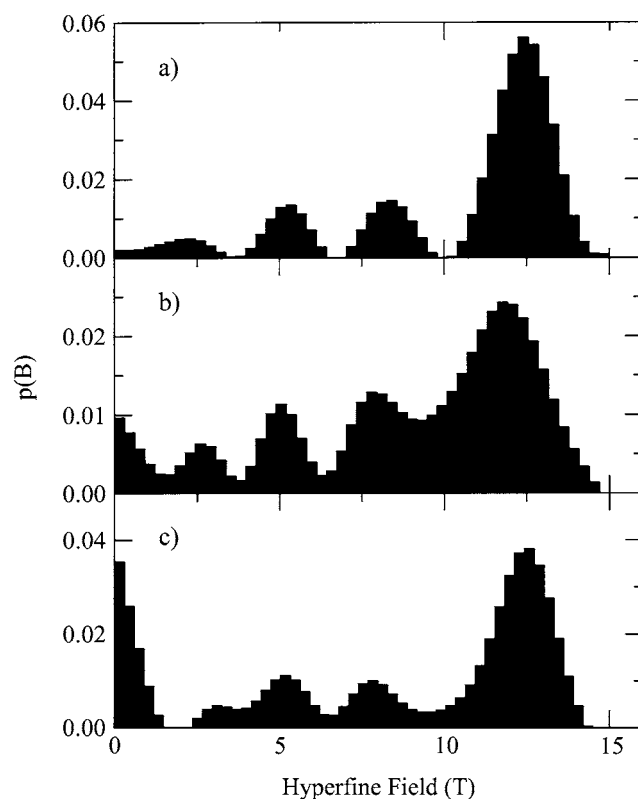
Figure 4. ^{119}Sn Mössbauer spectra recorded at 298 K from (a) 2% tin-doped α-Fe$_2$O$_3$ prepared by hydrothermal processing, (b) 3% tin-doped α-Fe$_2$O$_3$ prepared by mechanical milling, (c) 4% tin-doped α-Fe$_2$O$_3$ prepared by hydrothermal processing.

tin-containing precipitates contains tin ions in interstitial sites. Furthermore, the results reported here show that neither of the two structural models [6, 7] derived from diffraction techniques are totally adequate for describing the complexity of the local environment of tin in α-Fe$_2$O$_3$. It would appear that the microstructures are complex and depend on both the method of preparation and the tin content.

4.1. EXAFS

The Berry model [7], involving both interstitial and substitutional tin in the α-Fe$_2$O$_3$ matrix, seems to be superior in interpreting the EXAFS recorded from the materials made by both mechanical milling and hydrothermal processing. However, fitting by this model involved twelve free parameter, whereas the Jiang model [6] involved only seven free parameters. The lower R-values achieved in the former model may therefore not necessarily imply that this model is unambiguously correct, since an increased number of fitting parameters might be expected to result in a better fit. However, the reduced χ^2 values also shown in tables 1 and 2 do take into account the number of parameters refined in the model and thereby show that the Berry model [7] is a superior model to that of Jiang [6] when fitting the EXAFS data. The ratio of the first to second peak in the Fourier transform of the EXAFS recorded from the materials prepared by hydrothermal processing is indicative of more order in materials prepared by this

Figure 5. Magnetic field distributions obtained from [119]Sn Mössbauer spectra recorded at 298 K from (a) 2% tin-doped α-Fe$_2$O$_3$ prepared by hydrothermal processing, (b) 3% tin-doped α-Fe$_2$O$_3$ prepared by mechanical milling, (c) 4% tin-doped α-Fe$_2$O$_3$ prepared by hydrothermal processing.

method. The larger Debye–Waller factors associated with the fit of the EXAFS recorded from the materials prepared by mechanical milling also indicate enhanced disorder in such systems as a result of the method of preparation.

4.2. [119]Sn Mössbauer spectroscopy

At least three sextets and one doublet were needed to achieve a reasonable fit to the spectra recorded from samples made by ball milling and hydrothermal processing. The [119]Sn Mössbauer parameters of the doublet are similar to those of SnO$_2$, indicating that the samples may not be completely monophasic. The results showed the linewidths of the sextets in the spectra recorded from the sample made by ball milling to be considerably larger than those of the samples prepared by hydrothermal processing, and were therefore consistent with the EXAFS results in that they demonstrate a higher degree of disorder in the ball-milled sample.

The [119]Sn Mössbauer data failed to show any simple relationship between the peak area ratios in the spectra recorded from samples with different concentrations of tin and it is therefore difficult to use the data to distinguish between the two proposed models for the microstructure around tin in tin-doped α-Fe$_2$O$_3$. The field distribution (figure 5) implies a more complicated impact of disorder and vacancies on the hyperfine magnetic field at the tin nucleus than is assumed in either of the two models. From [119]Sn Mössbauer data, we conclude

that the local environment of tin in tin-doped α-Fe$_2$O$_3$ prepared by both mechanical milling and hydrothermal processing is more complex than implied by the two structural models derived from the x-ray powder diffraction data.

5. Conclusion

The model for tin-doped α-Fe$_2$O$_3$ involving a microstructure in which tin is located on both substitutional and interstitial sites in the corundum-related α-Fe$_2$O$_3$ structure [7] seems to be superior in interpreting the EXAFS recorded from materials made by both mechanical milling and hydrothermal processing. However, neither this model nor an alternative [6] involving the occupation by tin of only the interstitial sites in α-Fe$_2$O$_3$ are totally adequate for interpreting the complex [119]Sn Mössbauer spectra from tin doped α-Fe$_2$O$_3$ prepared by mechanical milling and hydrothermal processing. The EXAFS and [119]Sn Mössbauer spectra both provide evidence for a higher degree of disorder in material prepared by mechanical milling. The [119]Sn Mössbauer data indicate that both models are too simple to describe the local environment of tin in α-Fe$_2$O$_3$ and that the microstructural details are highly sensitive to tin content and the preparative method.

Acknowledgments

References

[1] Fabritchnyi P B, Lamykin E V, Babechkin A M and Nesmeianov A N 1972 *Solid State Commun.* **11** 343
[2] Schneider F, Melzer K, Mehner H and Deke G 1977 *Phys. Status Solidi* a **39** K115
[3] Takano M, Bando Y, Nakanishi N, Sakai M and Okinaka H 1987 *J. Solid State Chem.* **68** 153
[4] Music S, Popovic S, Metikos-Hukovic M and Gvozdic G 1991 *J. Mater. Sci. Lett.* **10** 197
[5] Kanai H, Mizutani H, Tanaka T, Funabiki T, Yoshida S and Takano M 1992 *J. Mater. Chem.* **2** 703
[6] Jiang J Z, Lin R, Nielson K, Mørup S, Rickerby D G and Clasen R 1997 *Phys. Rev.* B **55** 14 830
[7] Berry F J, Greaves C, McManus J G, Mortimer M and Oates G 1997 *J. Solid State Chem.* **130** 272
[8] Binsted N 1998 *EXCURV98* (CCLRC Daresbury Laboratory Computer Program)
[9] Wivel C and Mørup S 1981 *J. Phys. E: Sci. Instrum.* **14** 605